Journal of Alloys and Compounds 506 (2010) 103–108

Contents lists available at ScienceDirect

Journal of Alloys and Compounds

journal homepage: www.elsevier.com/locate/jallcom

Microstructural stability of zirconia–alumina composite coatings during hot corrosion test at 1050 °C

A. Keyvani, M. Saremi*, M. Heydarzadeh Sohi

School of Metallurgy and Materials, College of Engineering, University of Tehran, P.O. Box 11155-4563, Tehran, Iran

ARTICLE INFO

Article history:
Received 10 May 2010
Received in revised form 10 June 2010
Accepted 16 June 2010
Available online 25 June 2010

Keywords:
Hot corrosion
Zirconia–Alumina composite
Plasma spray

ABSTRACT

In the present work hot corrosion behavior of plasma sprayed zirconia–alumina coatings on Ni-base, IN-738, super alloy substrate was studied compared with normal zirconia. Hot corrosion resistance of the coatings was measured at 1050 °C using an atmospheric electrical furnace and a fused mixture of vanadium pentoxide and sodium sulfate salt.

The hot corrosion test duration was 4 h in each cycle, while the specimens were cooled in the furnace. The general and peripheral conditions of the specimens were inspected. If there were any cracks or spallation in coating wedge the test was stopped, the time was recorded and coating microstructure was studied. Composite coatings of zirconia–alumina having alumina as a top coat or a mixed zirconia–alumina layer, showed better resistance in hot corrosion tests. It was concluded that alumina overlay on zirconia has promoted the hot corrosion resistance of the coatings.

1. Introduction

The need to improve efficiency and higher energy output of energy generating systems caused the application of advanced materials. Coatings have a significant role towards this advance for the work pieces under high temperatures [1].

High temperature coatings are used to prevent surface degradations or as thermal barriers against warm atmosphere. The work pieces life span is controlled by their surface alterations thereby applying coatings significantly improves their performance and increase their durability. Surface alterations are usually done through corrosion, oxidation or erosion of solid particles. Simultaneous existence of these factors results in work piece strengthening drop in its ductility and eventual occurrence of its premature failure [2].

The extent of components requiring coatings is widely increasing especially in industrial and aero turbines [1,3,4].

Common thermal barrier coatings (TBCs), typically comprise a MCrAlY (M: nickel, cobalt or a mixture of these two) bond coat and a high temperature resistant yttria-stabilized zirconia (YSZ) top coat which is applied by thermal spray on super alloys surface [5]. The main disadvantage of TBCs is their decohesion from the bond coat which is caused by oxygen diffusion, oxidation and formation of thermally grown oxide (TGO) or infiltration of detrimental factors such as vanadium salts which results in phase transformation and spalling upon thermal cycling and high temperature oxidation [6–8]. In recent years layer composite of (Al_2O_3/YSZ) coatings on TBCs substrates have been proposed [9]. In these coatings due to existence of Al_2O_3 layer, oxygen or other detrimental factors infiltration is prevented and formations of TGO and zirconia phase transformation are retarded. In spite of the finding that thermal and mechanical properties of TBCs are improved by layer type composites [9], but the effect of other parameters such as type of composite is yet to be studied.

The aim of the present research is to investigate and make a comparison between common YSZ coating and a composite coating comprising of Al_2O_3/YSZ as top layer or Al_2O_3 as dispersed particles. In the present work, the coatings were applied by plasma spray, their hot corrosion behavior were studied and compared.

2. Experimental procedure

The base material was In-738 Ni super alloy in the shape of disks of 25 mm diameter and 10 mm thickness. Its composition is listed in Table 1.

Amdry 962 trade mark NiCrAlY micro-powders, Metco 204 NS-G trade mark YSZ zirconia powders and Metco 105 NS Al_2O_3 powders were prepared and coated using air plasma spray (APS) Metco 3 MB process. The specimens were shot blasted by 50–80 grain mesh alumina particles under 40–50 psi pressure before applying coatings. The surface oxides were removed using methyl ethyl kethon cleaner, and degreasing was performed under trichloro ethylene vapor. After washing they were preheated at 66–93 °C (<100 °C) and finally the following coatings were applied over the specimens. Argon was the primary and hydrogen was the secondary plasma gas and the plasma spray parameters are summarized in Table 2.

First NiCrAlY coating was plasma sprayed on the specimens with a thickness of 150 μm and then specimens were plasma sprayed with the following coatings:

* Corresponding author. Tel.: +98 21 61114117; fax: +98 21 66461024.
E-mail addresses: akeyvani@ut.ac.ir (A. Keyvani), saremi@ut.ac.ir (M. Saremi), mhsohi@ut.ac.ir (M. Heydarzadeh Sohi).

0925-8388/$ – see front matter © 2010 Published by Elsevier B.V.
doi:10.1016/j.jallcom.2010.06.110

Table 1
Chemical composition of IN738LC.

IN738LC	C	Al	Co	Cr	Mo	Nb	Ta	Ti	W	Ni
wt.%	0.101	3.45	8.32	16.09	1.70	0.75	1.73	3.34	2.56	Balance

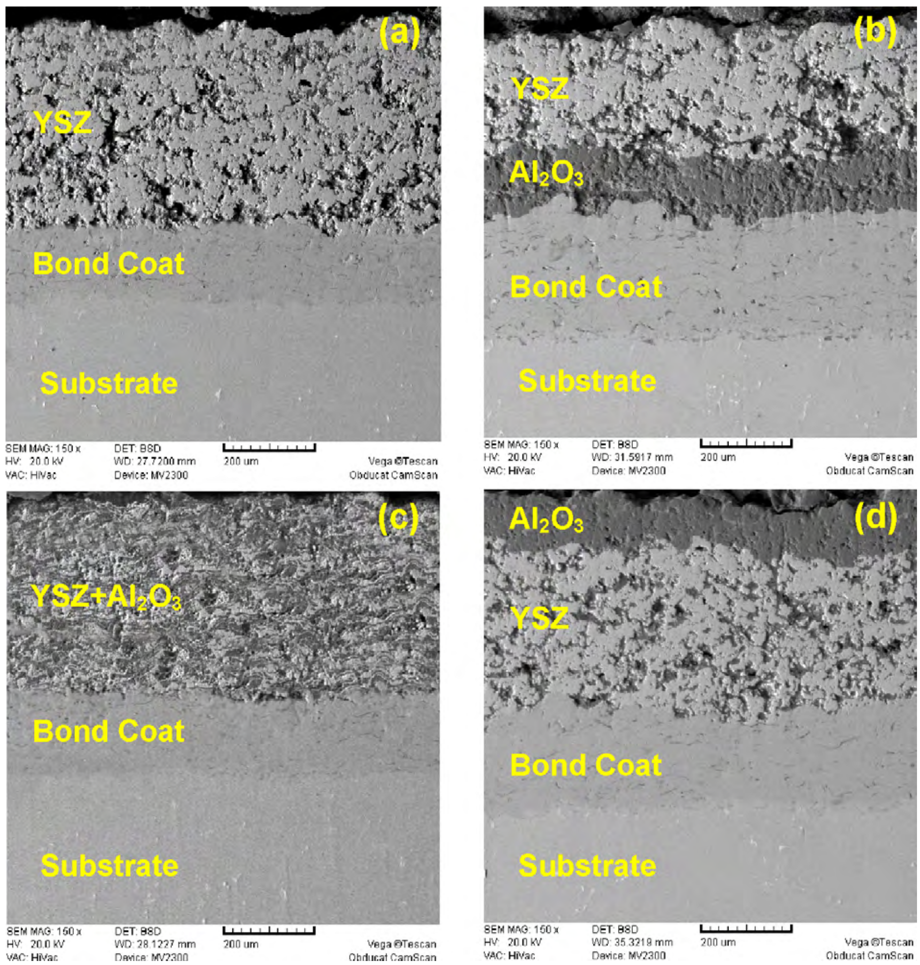

Fig. 1. Cross-sectional SEM images of as-sprayed coatings: (a) YSZ/NiCrAlY; (b) YSZ/Al_2O_3/NiCrAlY; (c) YSZ+Al_2O_3/NiCrAlY; and (d) Al_2O_3/YSZ/NiCrAlY.

(a) Usual YSZ with a thickness of 350 μm.
(b) A composite layer consisting of 100 μm of alumina on the bond coat then 250 μm top coat YSZ layer.
(c) A composite layer of Al_2O_3 and YSZ mixed powder in 350 μm thickness.
(d) A composite layer having 100 μm Al_2O_3 top coat and 250 μm YSZ.

YSZ + Al_2O_3 composite was made by mixing 60 wt.% of YSZ and 40 wt.% of Al_2O_3 powder in ball milled in alumina cup and balls in rotating speed of 150 rpm in 5 h.

Hot corrosion tests were carried out in an air furnace at 1050 °C in 4 h cycles in which the samples were furnace cooled. The surface was covered with 30 mg of a mixture of 55 wt.% V_2O_5 and 45 wt.% Na_2SO_4 salts per square centimeter of specimen's surfaces spreading in the way to keep 3 mm from the edge to avoid corrosive edge effect and form an even film of corrosive material on coating surface. The testing temperature and the concentration of corrosive materials were respectively selected according to zirconia phase transformation and performing a fast test.

The specimens were heated up from room temperature to 1050 °C. Leaved for each cycle, they were then inspected and their peripheral conditions were checked. If there were any cracks or spallation in coating edge the test was stopped and the time was recorded.

Optical microscopy (OM), scanning electronic microscopy (SEM, Oxford CAMSCAN-MV2300) equipped with energy dispersive spectrometer (EDS) and X-ray diffraction (XRD, Philips X'pert/Co-Kα radiation) were used to study the specimens.

Table 2
Plasma spray parameters for each coating.

Parameter	NiCrAlY	YSZ	YSZ + Al_2O_3	Al_2O_3
Current (A)	500	600	550	550
Voltage (V)	80	70	70	70
Primary gas flow, Ar (l/min)	55	40	40	40
Secondary gas flow, H_2 (l/min)	17	15	15	15
Powder feed rate (g/min)	42	37	37	37
Spray distance (mm)	130	120	100	100
Wheel rotation speed (rpm)	35	25	30	35

3. Results and discussions

The SEM image of the four types TBC layers microstructure is shown in Fig. 1. Some porosities can be observed in all coatings with exception of alumina top layer because it was made of fine alumina grains which is a characteristic of plasma sprayed coatings. The absence of void or microcracks in zirconia/alumina interface indicates proper cohesion of these two layers.

3.1. Hot corrosion test

The results of hot corrosion tests are listed in Table 3 in terms of appearance of the first visible crack on the surface. The Al_2O_3/YSZ composite coating revealed the most and YSZ/Al_2O_3 the least resistance to hot corrosion test. The low resistance of the latter may

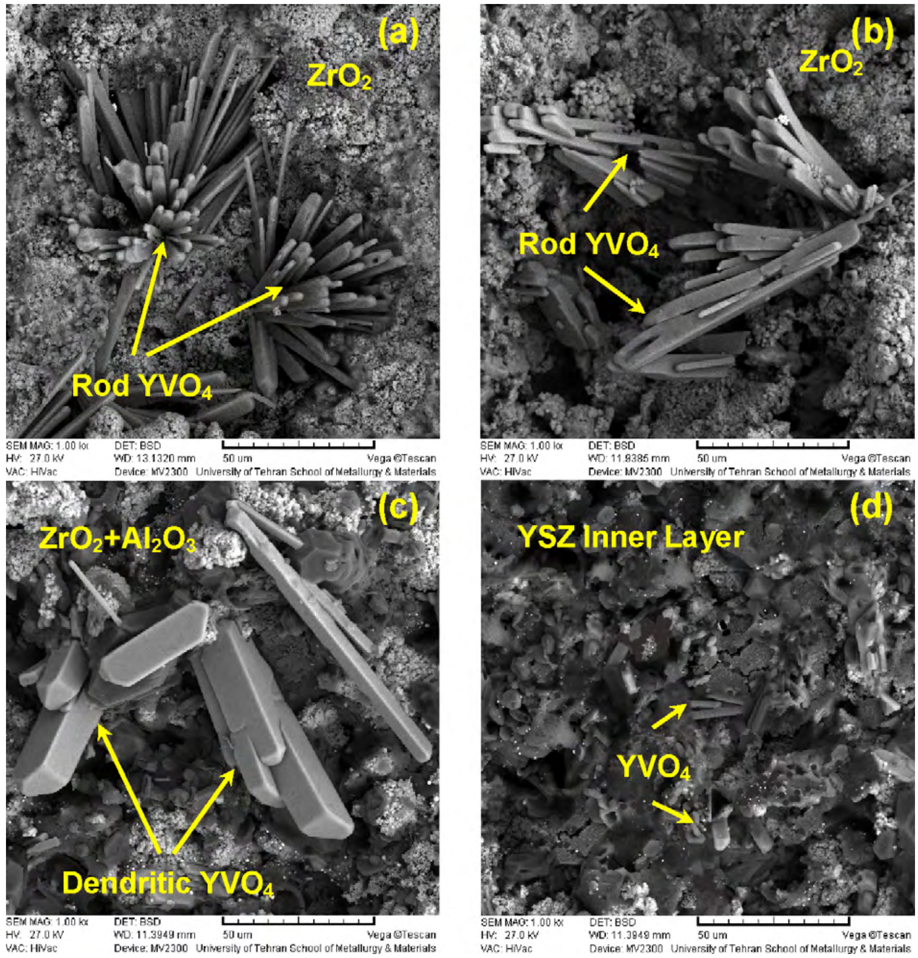

Fig. 2. Outer surface morphology of coatings: (a) YSZ/NiCrAlY; (b) YSZ/Al_2O_3/NiCrAlY; (c) YSZ+Al_2O_3/NiCrAlY; and (d) Al_2O_3/YSZ/NiCrAlY after hot corrosion test.

be attributed to the mismatch of thermal expansion of alumina and zirconia layers and also alumina with NiCrAlY intermediate layer.

The ordinary YSZ coating cracked after 16 h exposure to hot corrosion test. Composite YSZ + Al_2O_3 coating beared 24 h while in the Al_2O_3/YSZ composite coating, only alumina top coat dissented from zirconia after 40 h of exposure to hot corrosion and the composite YSZ/Al_2O_3 coating tolerated 12 h in hot corrosion test.

SEM micrographs from the coatings outer surfaces are illustrated in Fig. 2 and their cross-section microstructures after hot corrosion at 1050 °C is shown in Fig. 3. It is seen that the zirconia matrix became completely porous and some needle-like crystals of about 50 μm length grew outward from the zirconia matrix, which have different shapes in different coatings. These are corrosion products resulting from interaction between V_2O_5, yttria in the YSZ coatings. In composite Al_2O_3/YSZ coating the underneath zirconia layer remained almost unattacked. Outer surface morphology of zirconia coating after alumina top coat spallation is shown in Fig. 2d. Zirconia matrix and only some tiny needle crystals having a length of about 10 μm are noticeable in this figure.

The comparison of microstructures before and after hot corrosion of ordinary YSZ, YSZ/Al_2O_3 and YSZ + Al_2O_3 TBCs implies that

Table 3
The results of hot corrosion test at 1050 °C.

YSZ ordinary coating	Layer composite YSZ/Al_2O_3 coating	Particle composite Al_2O_3 + YSZ coating	Layer composite Al_2O_3/YSZ coating
4 cycles (16 h)	3 cycles (12 h)	6 cycles (24 h)	10 cycles (40 h)

outer surface of the coatings after hot corrosion becomes intensely porous because of the mentioned needle-like crystals formed on the surface (Fig. 2a–c). The shape of these crystals in YSZ, YSZ/Al_2O_3 coatings is needle-like and they grow outwards but in YSZ + Al_2O_3 coating it is dendritic (sprout-like). The XRD analysis from the surface of the coatings after hot corrosion reveals monoclinic zirconia and tetragonal zirconia which existed also in as-sprayed coating and YVO_4 composition.

Fig. 3 shows cross-sectional images of the coatings after hot corrosion test. All coatings are separated from the bond coat/YSZ interface except in Al_2O_3/YSZ composite coating in which in spite of the spallation of Al_2O_3 the underneath YSZ remained unattacked. Thus one can say that in comparison with other three coatings, layer composite of Al_2O_3/YSZ coating is much more resistant to hot corrosion in which the alumina overlay played an important role in decreasing the infiltration of molten materials into zirconia layer. Composite YSZ/Al_2O_3 coating showed the least endurance against hot corrosion test, i.e., 12 h resistance.

The X-ray analysis of the needle type crystals, shown in Fig. 2, is demonstrated in Fig. 4. It is seen that the crystals were composed of yttrium, vanadium and oxygen, and their XRD analysis confirmed that the composition is YVO_4. It seems that during hot corrosion, yttrium element has been removed from YSZ coating by interaction with vanadium oxide.

3.2. Phase analysis

Fig. 5 shows the existing phases in the surface of TBC coating after hot corrosion at 1050 °C. The overlay YSZ layer coating

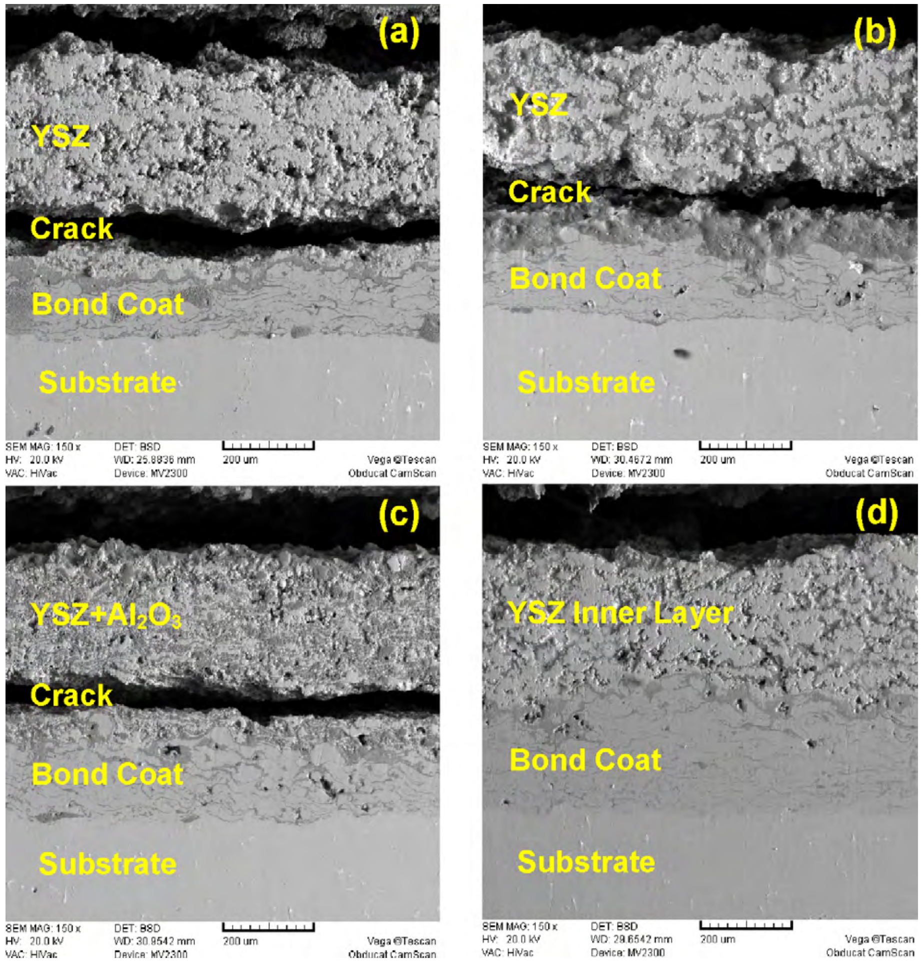

Fig. 3. Cross-sectional SEM images of TBC coatings: (a) YSZ/NiCrAlY; (b) YSZ/Al_2O_3/NiCrAlY; (c) YSZ+Al_2O_3/NiCrAlY; and (d) Al_2O_3/YSZ/NiCrAlY after hot corrosion test.

has the tetragonal zirconia as the main phase and also the new phases of monoclinic zirconia and tetragonal YVO_4 composition which can be regarded as corrosion products are observed. Phase analysis of composite YSZ + Al_2O_3 coating indicated that it contains rhombohedral (α) and orthorombic (δ) alumina and also tetragonal and monoclinic zirconia phases as well as YVO_4 composition. In Al_2O_3/YSZ composite coating, in which Al_2O_3 top coat spalled from the specimen surface after hot corrosion, in addition to the tetragonal zirconia as the main phase, phases of monoclinic zirconia and tetragonal YVO_4 composition have also formed as corrosion products but the decrease in peak intensities is due to the decrease in corrosion effect.

Morphology of YSZ layer surface after Al_2O_3 layer spallation (Fig. 2d) consists of some small crystals. XRD analysis from

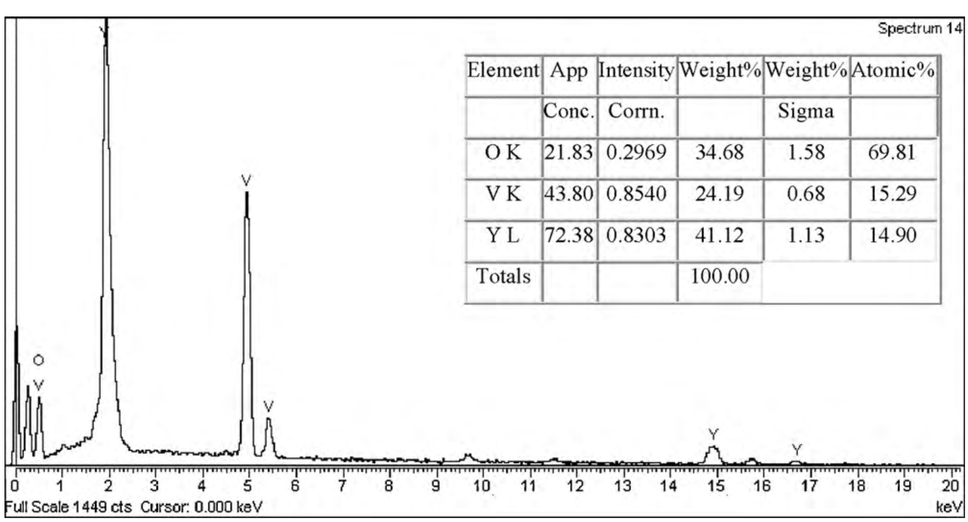

Element	App	Intensity	Weight%	Weight%	Atomic%
	Conc.	Corrn.		Sigma	
O K	21.83	0.2969	34.68	1.58	69.81
V K	43.80	0.8540	24.19	0.68	15.29
Y L	72.38	0.8303	41.12	1.13	14.90
Totals			100.00		

Fig. 4. Spot EDS spectrum of needle and dendritic crystals shown in Fig. 2a–d.

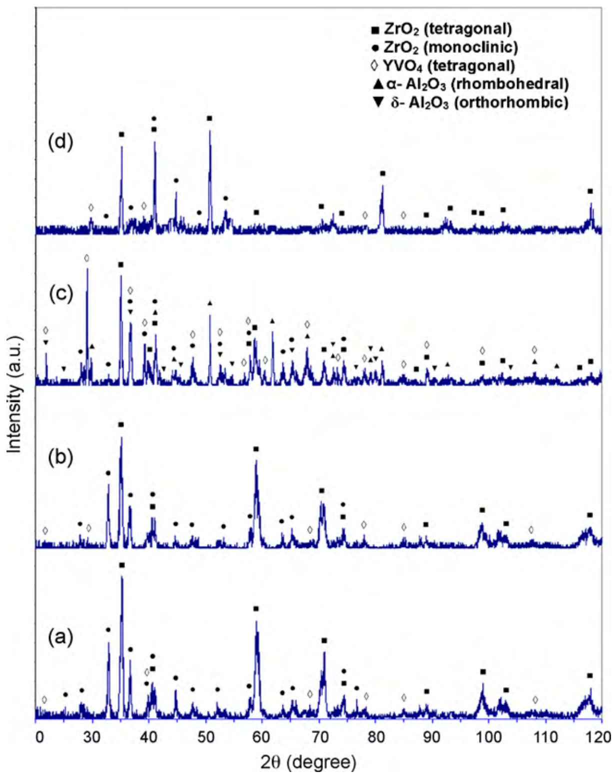

Fig. 5. X-ray diffraction patterns of coatings outer surface: (a) YSZ/NiCrAlY; (b) YSZ/Al_2O_3/NiCrAlY; (c) YSZ + Al_2O_3/NiCrAlY; and (d) Al_2O_3/YSZ/NiCrAlY after hot corrosion.

mentioned surface reveals monoclinic zirconia phase and YVO_4 composition too but peak intensities of aforesaid compositions in comparison with ordinary YSZ, YSZ/Al_2O_3 and YSZ + Al_2O_3 have significantly dropped. Since the percent of formation of monoclinic zirconia unstable phase is so important in hot corrosion process, Eq. (1) is used to determine monoclinic phase volume fraction [10–16]:

$$M\% = \frac{M_1 + M_2}{M_1 + M_2 + T} \quad (1)$$

where T is the intensity peak of tetragonal zirconia at (1 0 1) plane, M_1 is the intensity peak of monoclinic zirconia at $(\bar{1}\,1\,1)$ plane and M_2 is the intensity peak of monoclinic zirconia at (1 1 1) plane in XRD plots after hot corrosion. Fig. 6 shows that the percentage of undesirable monoclinic YSZ in all the tested composites coatings calculated using formula (1). Thus it is clear that content of monoclinic zirconia in ordinary TBCs and YSZ/Al_2O_3 coatings, is maximum and it is minimum in Al_2O_3/YSZ. The monoclinic zirconia is unstable and transforms to tetragonal phase at a temperature of about 1000 °C where during cooling process it converts to monoclinic again with 3–5% volume change [10,17] which is responsible for the spallation of the coating during thermal cycles. The mechanism of monoclinic zirconia formation during hot corrosion is based on the following reactions [18]:

$$V_2O_5 + Na_2SO_4 \rightarrow 2(NaVO_3) + SO_3 \quad (2)$$

$$ZrO_2(Y_2O_3) + 2(NaVO_3) \rightarrow ZrO_2(\text{monoclinic}) + 2YVO_4 + Na_2O \quad (3)$$

At first according to Eq. (2), sodium vanadate ($NaVO_3$) is formed. Then according to Eq. (3), $NaVO_3$ reacts with zirconia stabling component (Y_2O_3) to form monoclinic ZrO_2, YVO_4 and Na_2O. The Na_2O compound in Eq. (3) is assumed to be sublimated during hot corrosion test [19–29].

Proper results of Al_2O_3/YSZ coating during oxidation and hot corrosion state that alumina top coat decreases oxygen diffusion towards NiCrAlY bond coat and acts as a strong barrier against the infiltration of corrosive materials into the ceramic YSZ. As a result the existence of Al_2O_3 top coat on YSZ coating can increase TBC life span under service conditions of gas turbine blades.

4. Conclusions

Based on the results of the present work it can be concluded that composite coating with alumina can improve hot corrosion resistance of YSZ at 1050 °C in the presence of V_2O_5 and Na_2SO_4.

Al_2O_3/YSZ was the most resistant coating during exposure to hot corrosion. This is because dense alumina layer significantly prevented the infiltration of molten salt (V_2O_5 + Na_2SO_4) into YSZ layer.

Spallation of YSZ which is partly due to the interaction of V_2O_5 with yttria can be retarded if Al_2O_3 is used as a top layer coat on YSZ or mixed with YSZ.

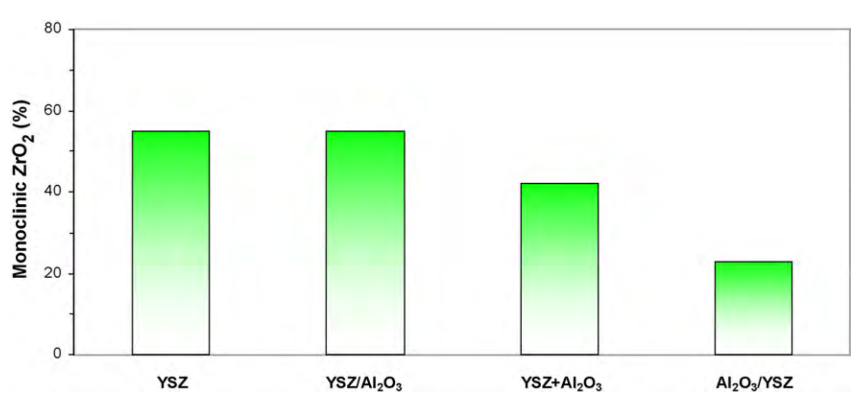

Fig. 6. Approximate percentage (content) of monoclinic zirconia in TBC coatings after hot corrosion test.

References

[1] J.R. Davis, "Protective Coatings for Superalloys", ASM Specially Handbook, Heat-Resistance Materials, ASM International Materials Park, Ohio, 1997, pp. 335–344.
[2] G.N. Goward, L.L. Seigle, Diffusion Coatings for Gas Turbine Engine Hot Section Parts", Metals Handbook, vol. 5, 10th ed., ASM International Materials Park, Ohio, 1994, pp. 611–617.
[3] A.N. Khan, J. Lu, H. Liao, Surface and Coatings Technology Vol.168 (2003) 291–299.
[4] J. Wirgen, L. Pejryd, Proceeding of the 15th International Thermal Spray Conference, Nice, France, 1998, pp. 1531–1541.
[5] X.Q. Cao, R. Vassenb, D. Stoeverb, European Ceramic Society 24 (2004) 1–10.
[6] M.J. Pomeroy, Materials and Design 26 (2005) 223–231.
[7] U. Schulz, C. Leyens, K. Fristscher, M. Peters, B.S. Brings, O. Lavigne, J.M. Dorvaux, M. Poulain, R. Mevrel, M. Caliez, Aerospace Science and Technology 7 (2003) 73–80.
[8] N.P. Padture, M. Gell, L. Eric, H. Jordan, Materials Science and Engineering 296 (2002) 280–285.
[9] M. Saremi, A. Afrasiabi, A. Kobayashi, Surface and Coatings Technology 202 (2008) 3233–3238.
[10] K.N. Strafford, P.K. Datta, J.S. Gray, Surface Engineering Practice, Ellis Horwood Limited, 1990, pp. 4–9, 259–260.
[11] X. Lin, Y. Zeng, X. Zhou, C. Ding, Materials Science and Engineering A 357 (2003) 228–234.
[12] L.L. Shaw, D. Goberman, R. Ren, M. Gell, S. Jiang, Y. Wang, T.D. Xiao, P.R. Strutt, Surface and Coatings Technology 130 (2000) 1–8.
[13] G. Bolelli, V. Cannillo, I. Lusvarghi, T. Manfredini, Surface and Coatings Technology 201 (2006) 458–473.
[14] P.C. Tsai, J.H. Lee, C.S. Hsu, Surface and Coatings Technology 201 (2007) 5143–5147.
[15] J.R. Brandon, R. Taylor, Surface and Coatings Technology 46 (1991) 91–101.
[16] C. Batista, A. Portinha, R.M. Ribeiro, V. Teixeira, C.R. Oliveira, Surface and Coatings Technology 200 (2006) 6783–6791.
[17] S.V. Joshi, M.P. Srivastava, Surface and Coatings Technology 56 (1993) 215–224.
[18] I. Gurrappa, Materials Science Letters 17 (1998) 1267–1269.
[19] R.C. Weast, CRC Handbook of Chemistry and Physics, 58th ed., CRC Press, Ohio, 1978, pp. B-162, B-174.
[20] H.C. Chen, Z.Y. Liu, Y.C. Chuang, Thin Solid Films 223 (1992) 56–64.
[21] M.P. Boyce, Gas Turbine Engineering Handbook, Gulf Publishing Company, Houston, Texas, 1992, pp. 317–318.
[22] C. Ramachandra, K.N. Lee, S.N. Tewari, Surface and Coatings Technology 172 (2003) 150–157.
[23] S.Y. Park, J.H. Kim, M.C. Kim, H.S. Song, C.G. Park, Surface and Coatings Technology 190 (2005) 357–365.
[24] M. Gell, E. Jordan, K. Vaidyanathan, K.M. Carron, Surface and Coatings Technology 120–121 (1999) 53–60.
[25] A. Afrasiabi, Application of plasma sprayed YSZ-Al_2O_3 composite TBC on Ni-based Super alloy (IN-738) and evaluation of the microstructure and its thermal stability, PhD Thesis, Under supervision of Dr. M. Saremi, University of Tehran, 2008.
[26] H.D. Steffens, Kaczmark, Welding in the World 28 (1990) 224–230.
[27] P. Strunz, G. Schumacher, R. Vassen, A. Wiedenmann, Acta Materialia 52 (2004) 3305–3312.
[28] J.R. Mawdsley, Y.J. Su, K.T. Faber, T.F. Bernecki, Materials Science and Engineering A 308 (2001) 189–199.
[29] L.A. Lay, Corrosion Resistance of Technical Ceramics, 2nd ed., HMSO, London, 1991, pp. 83–84.